

Free vibration of Levy-type rectangular laminated plates using efficient zig-zag theory

Susanta Behera^a and Poonam Kumari*

*Department of Mechanical Engineering, Indian Institute of Technology Guwahati,
Guwahati-781039, Assam, India*

(Received December 18, 2017, Revised January 15, 2018, Accepted January 17, 2018)

Abstract. First time, an exact solution for free vibration of the Levy-type rectangular laminated plate is developed considering the most efficient Zig-Zag theory (ZIGT) and third order theory (TOT). The plate is subjected to hard simply supported boundary condition (Levy-type) along x axis. Using the equilibrium equations and the plate constitutive relations, a set of 12 m first order differential homogenous equations are obtained, containing displacements and stress resultant as primary variables. The natural frequencies of a single-layer isotropic, multi-layer composites and sandwich plates are tabulated for three values of length-to-thickness ratio (S) and five set of boundary conditions and further assessed by comparing with existing literature and recently developed 3D EKM (extended Kantorovich method) solution. It is found that for the symmetric composite plate, TOT produces better results than ZIGT. For antisymmetric and sandwich plates, ZIGT predicts the frequency for different boundary conditions within 3% error with respect to 3D elasticity solution while TOT gives 10% error. But, ZIGT gives better predictions than the TOT concerning the displacement and stress variables.

Keywords: zig-zag theory; analytical solution; levy-type; free vibration; sandwich plate; composite plate

1. Introduction

In recent years, laminated composite structures are extensively used in some of the weight sensitive and sophisticated engineering applications such as in aerospace, civil, mechanical and naval industries where these structures are subjected to various loadings (static and dynamic loads) and boundary conditions. Unlike the isotropic plate structures, composite laminates experience different couplings among bending, extension and twisting pertaining to its varied stacking order among the layers. Hence, the development of a computationally easy, efficient and reliable dynamic analysis of laminated plates has been the topic of research since last few decades. The two-dimensional (2D) theories are preferred for the design and optimization of laminated structures as it is relatively simple and easy to execute in comparison to 3D solutions with reasonable accuracy. To address the above concern, 2D theories of varying computational efficiency and accuracy are available in abundance for laminated plates which can broadly be

*Corresponding author, Ph.D. E-mail: kpmech@iitg.ernet.in

^aPh.D. Student E-mail: susantabc@gmail.com

classified as equivalent single layer (ESL) theories, refined/modified single layer (RESL) theories, layerwise theories (LWT) and zig-zag theories (ZIGT). In recent review articles (Sayyad and Ghugal 2015, Caliri *et al.* 2016, Sayyad and Ghugal 2017), elaborate reviews of 2D plate theories are presented considering various computational methods on static as well as free vibration analysis of different laminated composite and sandwich structures. Analytical solutions are preferred over numerical solutions for better accuracy and simplicity.

Leissa and his coworkers (Leissa 1973, Leissa and Kang 2002) presented the free vibration analysis of plate based on the classical laminate plate theory (CLPT), which is based on Kirchhoff's hypothesis, where the transverse normal and shearing effects are neglected. Hence, the CLPT provides good results for thin plates, while in other hand it over-predicts the natural frequencies and under-predicts the deflections for moderately thick isotropic/composite plates. Then, the first order shear deformation theory (FSDT) is proposed for moderately thick plates (Reissner 1945, Mindlin 1951) to overcome the deficiency of CLPT. The FSDT does not satisfy the shear traction free conditions at the top and bottom surfaces of the plates, therefore a shear correction factor is required in FSDT in order to satisfy the transverse shear traction free conditions on the top and bottom surfaces of the plate. Based on FSDT, the vibration response of laminated composite plates are presented in references (Xiang and Wei 2004, Hashemi and Arsanjani 2005, Ferreira *et al.* 2005, Ferreira *et al.* 2009, Thai and Choi 2013). Though, FSDT is good in predicting the vibration responses with reasonable accuracy for thin and moderately thick plates, but its dependence on appropriate choice of shear correction factor makes it inconvenient for accurate analysis of thick plates. The limitations of FSDT are overcome by the development of higher order shear deformation theories (HSDT) which involves the transverse shear stress function. The HSDT is applied to study the behaviour of laminated composite and sandwich plates for buckling and vibration (Noor 1973, Kant and Swaminathan 2001, Akavci and Tanrikulu 2008, Swaminathan and Patil 2008, Meiche *et al.* 2011, Mantari *et al.* 2011, Mahi *et al.* 2015) cases. Based on a global HSDT, Matsunaga presented the free vibration analysis of cross-ply (Matsunaga 2000) and angle-ply (Matsunaga 2001) laminated composite plates taking into account the effects of shear deformations and rotary inertia. However, the above advanced two-dimensional (2D) laminate theories were assessed for their accuracy against the 3D solutions of plates subjected to Navier-type supports (all round simply supported boundary conditions). Such an assessment can not provide the complete evaluation of theories because boundary effects are absent for the simply-supported edges (Karama *et al.* 1993). Very limited research articles have been published for both static and dynamic analysis of laminated plates considering the Levy-type support conditions.

Analytical free vibration solutions for elastic rectangular laminated plates with Levy-type boundary conditions have been presented for symmetric cross-ply (Khdeir 1988) and unsymmetric cross-ply plates (Khdeir 1989) and for both static and free vibration analysis of symmetric cross-ply plates (Chen and Liu 1990) based on the FSDT. Khdeir and Librescue (1988) presented free vibration and buckling analysis of symmetric cross-ply laminated elastic plates using a higher-order theory. Liew (1996) presented the free vibration of thick symmetric laminates using Ritz solution. Recently, Hashemi *et al.* (2011) presented exact solutions for free vibration of Levy-type rectangular thick plates via Reddy's third-order shear deformation plate theory. Numerical results are presented for single layer isotropic plate. Thai and Kim (2012) presented the free vibration analysis of single-layer Levy-type orthotropic plate based on two variable refined plate theory (RPT). Very recently, Thai *et al.* (2017) presented a new simple higher order shear deformation plate theory for static and free vibration analysis of plates based on RPT and 3D

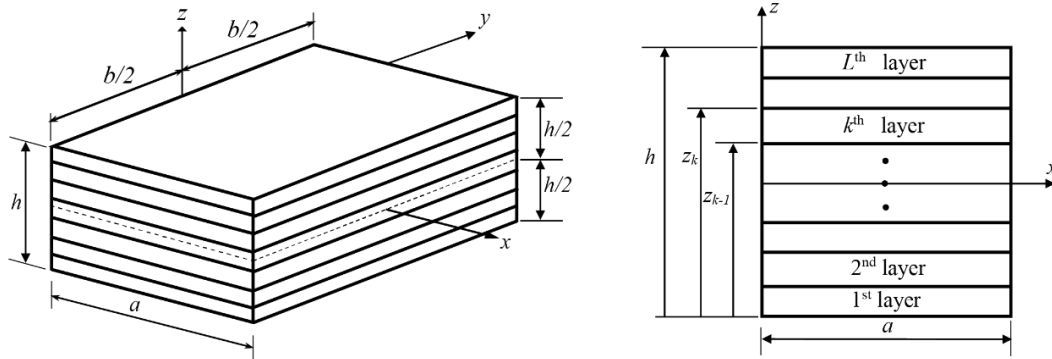


Fig. 1 Geometry of the laminated plate

elasticity theory. In this paper also, numerical results are presented for the isotropic plate.

The efficient layerwise zig-zag theory (ZIGT) proposed by Kapuria and Kulkarni (2007) for laminated structures, has emerged as the best possible compromise between the accuracy and computational efficiency. The in-plane displacements in this theory are assumed to have a layerwise linear variation with a global third order variation across the thickness. But the number of displacement variables is reduced to only five, as in the smeared theory like the first order shear deformation theory (FSDT) and third order theory (TOT), by enforcing the conditions of transverse shear stress continuity at layer interfaces and zero shear traction at the top and bottom surfaces. Recently, Kumari and Kapuria (2011) presented the static analysis of rectangular cross-ply Levy-type plates using zig-zag theory employing the mixed formulation approach. As per the author's knowledge, there exist no free vibration analysis of composite and sandwich plates based on efficient zig-zag theory subjected to Levy-type boundary conditions. The aim of this paper is to present the exact analytical free vibration solution for Levy-type composite and sandwich plates. The natural frequencies and mode shapes for different boundary conditions are obtained for plates with varied cross-ply lay-ups. Effect of inplane modulus ratios and span-to-thickness ratios on the plate natural frequencies are evaluated and discussed. As a special case of ZIGT, the TOT solution is also developed and both the results are with the 3D exact results for simply supported case and with the 3D EKM results for other type of boundary conditions. The numerical results are estimated and presented for the laminated composite and sandwich plates which will help to assess the accuracy of other numerical solutions. The results from this theory are compared with the previously published results and found to be in good agreement.

2. Mathematical modelling

2.1 Geometry

Let us consider, a multilayered orthotropic rectangular plate of dimensions $(a \times b \times h)$ along x , y and z -axis, respectively as illustrated in Fig. 1. The principal material direction x_3 is parallel to reference axis z whereas other material directions x_1 and x_2 can make 0° or 90° to the inplane reference axes x , y . The plies are numbered from the bottom (1st layer) to top (L th layer). The z coordinate of the bottom and top surface of k th ply is denoted as $z = z^{k-1}$ and $z = z^k$, respectively.

The plate is subjected to hard simply supported along x -axis (i.e., $x = 0$ and $x = a$) while along y -axis (i.e., $y = -b/2$ and $y = +b/2$), any combination among clamped, free and simply supported boundary conditions can be applied. The mid-plane (x - y) of the plate is chosen as a reference plane ($z = 0$).

2.2 The strain-displacement and constitutive relations

The linear strain displacement relations of the orthotropic elastic laminate with respect to the plate axis system (x - y - z) are considered as

$$\begin{aligned}\varepsilon_x &= u_{x,x}, & \varepsilon_y &= u_{y,y}, \\ \gamma_{yz} &= u_{y,z} + w_{,y}, & \gamma_{zx} &= u_{x,z} + w_{,x}, & \gamma_{xy} &= u_{x,y} + u_{y,x}\end{aligned}\quad (1)$$

The linear constitutive relations of the orthotropic elastic laminate with the usual assumption of negligible transverse normal stress ($\sigma_z = 0$) are as given below

$$\begin{aligned}\sigma_x &= Q_{11}\varepsilon_x + Q_{12}\varepsilon_y, & \sigma_y &= Q_{12}\varepsilon_x + Q_{22}\varepsilon_y, \\ \tau_{yz} &= Q_{44}\gamma_{yz}, & \tau_{zx} &= Q_{55}\gamma_{zx}, & \tau_{xy} &= Q_{66}\gamma_{xy}\end{aligned}\quad (2)$$

where $\varepsilon_x, \varepsilon_y$ are normal strains, σ_x, σ_y are normal stresses, $\gamma_{xy}, \gamma_{yz}, \gamma_{zx}$ are shear strains, $\tau_{xy}, \tau_{yz}, \tau_{zx}$ are shear stresses and $Q_{ij} (i, j = 1, 2, \dots, 6)$ are the elements of reduced stiffness matrix.

2.3 Kinematics assumptions

The displacements components u_α ($\alpha = x, y$) and w are considered along x, y and z directions, respectively. The inplane displacements u_α are approximated as a combination of a third-order variation in z over the entire laminate thickness and a layerwise linear variation with discontinuity in slopes $u_{\alpha,z}$ (subscript comma means differentiation) at the layer interface. The out-of-plane displacement, w is assumed to be uniform across the thickness (Kapuria and Kulkarni 2007).

$$u_\alpha(x, y, z, t) = u_{k_\alpha}(x, y, t) - zw_{0,\alpha}(x, y, t) + z\psi_{k_\alpha}(x, y, t) + z^2\xi_\alpha(x, y, t) + z^3\eta_\alpha(x, y, t) \quad (3a)$$

$$w(x, y, z, t) = w_0(x, y, t) \quad (3b)$$

Here, u_{k_α} denotes the translation components of the k th layer and ψ_{k_α} corresponds to its shear rotation, which has a piecewise linear variation across the layers. ξ_α and η_α are the quadratic and cubic terms in z , which have cubic global variation through the thickness. Using the $2(L-1)$ number of conditions, each for the continuity of u_α and the transverse shear stresses τ_{ij} ($i, j = x, y, z$) at the layer interfaces and the four shear traction-free conditions at the top and bottom surfaces at $z = z_0, z_L$, the $(4L+4)$ variables $u_{k_\alpha}, \psi_{k_\alpha}, \xi_\alpha$ and η_α in Eq. (3a), are expressed in terms of variables u_{0_α} and ψ_{0_α} to yield

$$u_\alpha(x, y, z, t) = u_{0_\alpha}(x, y, t) - zw_{0,\alpha}(x, y, t) + \mathbf{R}^k(z)\psi_{0_\alpha}(x, y, t) \quad (4)$$

for $z_{k-1} \leq z \leq z_k$, where $\mathbf{R}^k(z)$ is a 2×2 matrix of layerwise functions of z of the form.

$$\mathbf{R}^k(z) = \mathbf{R}_1^k + z\mathbf{R}_2^k + z^2\mathbf{R}_3 + z^3\mathbf{R}_4 \quad (5)$$

$\mathbf{R}_1^k, \mathbf{R}_2^k, \mathbf{R}_3$ and \mathbf{R}_4 are 2×2 coefficient matrices which rely on the properties of plate material and the stacking order and their expressions are given in Ref. (Kapuria and Kulkarni 2007).

In the smeared third order theory (TOT), the layerwise terms u_{k_α} and ψ_{k_α} in Eq. (3a) are replaced by u_{0_α} and ψ_{0_α} . The inplane displacements, u_α can be expressed using Eq. (4) with $\mathbf{R}^k(z)$ being replaced by the global function $\mathbf{R}(z)$ for all layers after satisfying the traction free conditions at both the top and bottom surfaces as

$$\mathbf{R}(z) = [z - 4z^3 / 3h^2] \mathbf{I}_2 \quad (6)$$

Where \mathbf{I}_2 is 2×2 unity matrix. Eqs. (3b) and (4) are substituted into Eq. (1) to yield

$$\begin{aligned} \varepsilon_x &= u_{0,x,x} - zw_{0,xx} + R_{11}^k \psi_{0,x,x} + R_{12}^k \psi_{0,y,x} \\ \varepsilon_y &= u_{0,y,y} - zw_{0,yy} + R_{21}^k \psi_{0,x,y} + R_{22}^k \psi_{0,y,y} \\ \gamma_{xy} &= u_{0,x,y} + u_{0,y,x} - 2zw_{0,xy} + R_{21}^k \psi_{0,x,x} + R_{11}^k \psi_{0,x,y} + R_{22}^k \psi_{0,y,x} + R_{12}^k \psi_{0,y,y} \\ \gamma_{yz} &= R_{21,z}^k \psi_{0,x} + R_{22,z}^k \psi_{0,y} \\ \gamma_{zx} &= R_{11,z}^k \psi_{0,x} + R_{12,z}^k \psi_{0,y} \end{aligned} \quad (7)$$

3. Equations of equilibrium and boundary conditions

The Hamilton's principle for the elastic medium can be expressed, using the notation

$\langle \dots \rangle = \sum_{k=1}^L \int_{z_{k-1}^+}^{z_k^-} (\dots) dz$ for integration across the thickness as

$$\begin{aligned} \int_t \int_A [\langle \rho \ddot{u}_x \delta u_x + \rho \ddot{u}_y \delta u_y + \rho \ddot{w} \delta w + \sigma_x \delta \varepsilon_x + \sigma_y \delta \varepsilon_y + \tau_{xy} \delta \gamma_{xy} + \tau_{yz} \delta \gamma_{yz} + \tau_{zx} \delta \gamma_{zx} \rangle] dA dt \\ - \int_t \int_{\Gamma_L} \langle \sigma_n \delta u_n + \tau_{ns} \delta u_s + \tau_{nz} \delta w \rangle ds dt = 0 \end{aligned} \quad (8)$$

where A denotes the surface of the mid-plane area of the plate and Γ_L represents the mid-plane boundary curve of the plate with normal and tangent as n and s , respectively. The variational equation is expressed in terms of $\delta u_0, \delta w_0$ and $\delta \psi_0$, to yield the governing equations and boundary conditions.

3.1 Inertia matrices

Eqs. (4) and (3b) for u and w can be expressed as

$$u_\alpha = f_1(z) \bar{u}_1, \quad w = f_2(z) \bar{u}_2 \quad (9a)$$

$$\delta u_\alpha = f_1(z)\bar{u}_1, \quad \delta w = f_2(z)\delta\bar{u}_2 \quad (9b)$$

with

$$\begin{aligned} \bar{u}_1 &= [u_0^T \quad -w_{0,d}^T \quad \psi_0^T]^T = [u_{0,x} \quad u_{0,y} \quad -w_{0,x} \quad -w_{0,y} \quad \psi_{0,x} \quad \psi_{0,y}], \\ f_1(z) &= [\mathbf{I}_2 \quad z\mathbf{I}_2 \quad \mathbf{R}_k^z]^T, \quad f_2(z) = [1]^T \end{aligned}$$

The inertia terms in Eq. 8 can be expressed as

$$\begin{aligned} \langle \rho \delta u^T \ddot{u} + \rho \delta w \ddot{w} \rangle &= \langle \rho \delta \bar{u}_1^T f_1^T(z) f_1(z) \ddot{\bar{u}}_1 + \rho \delta \bar{u}_2^T f_2^T(z) f_2(z) \ddot{\bar{u}}_2 \rangle \\ &= \delta \bar{u}_1^T (\ddot{\bar{u}}_1) + \delta \bar{u}_2^T (\ddot{\bar{u}}_2) \end{aligned} \quad (10)$$

where the inertia matrices I and \bar{I} are of size 6×6 and 1×1 and defined as

$$I = \langle \rho f_1^T(z) f_1(z) \rangle, \quad \bar{I} = \langle \rho f_2^T(z) f_2(z) \rangle \quad (11)$$

3.2 Stress resultants

Substituting Eq. (4) and (3b) for displacements (u_x, u_y, u_z) and Eq. (7) for strain components ($\varepsilon_x, \varepsilon_y, \gamma_{xy}, \gamma_{yz}, \gamma_{zx}$) into Eq. (8) yields

$$\begin{aligned} &\int_t \int_A [N_x \delta u_{0,x,x} + N_y \delta u_{0,y,y} + N_{xy} (\delta u_{0,x,y} + \delta u_{0,y,x}) - M_x w_{0,xx} - M_y w_{0,yy} - 2M_{xy} w_{0,xy} \\ &+ P_x \delta \psi_{0,x,x} + P_{yx} \delta \psi_{0,x,y} + P_{xy} \delta \psi_{0,y,x} + P_y \delta \psi_{0,y,y} + Q_x \delta \psi_{0,x} + Q_y \delta \psi_{0,y}] dA \\ &- \int_{\Gamma_L} [N_n \delta u_{0,n} + N_{ns} \delta u_{0,s} - M_n \delta w_{0,n} + (V_n + M_{ns,s}) \delta w_0 + P_n \delta \psi_{0,n} + P_{ns} \delta \psi_{0,s}] [ds] dt \\ &- \sum_i \Delta M_{ns}(s_i) \delta w_0(s_i) = 0 \end{aligned} \quad (12)$$

where the lateral surface has corners at $s = s_i$. The inplane stress resultants (N_x, N_y, N_{xy}), bending moments (M_x, M_y, M_{xy}), higher order moments (P_x, P_{yx}, P_{xy}), shear resultants (Q_x, Q_y) and Kirchhoff shear resultants (V_x, V_y), are defined in the expanded form as given below

$$\begin{aligned} \begin{bmatrix} N_x \\ N_y \\ N_{xy} \\ M_x \\ M_y \\ M_{xy} \\ P_x \\ P_{yx} \\ P_{xy} \\ P_y \end{bmatrix} &= \begin{bmatrix} A_{11} & A_{12} & \cdots & A_{1,10} \\ A_{21} & A_{22} & \cdots & A_{2,10} \\ \vdots & \vdots & \vdots & \vdots \\ A_{10,1} & A_{10,2} & \cdots & A_{10,10} \end{bmatrix} \begin{bmatrix} u_{0,x,x} \\ u_{0,y,y} \\ u_{0,x,y} + u_{0,y,x} \\ -w_{0,xx} \\ -w_{0,yy} \\ -2w_{0,xy} \\ \psi_{0,x,x} \\ \psi_{0,x,y} \\ \psi_{0,y,x} \\ \psi_{0,y,y} \end{bmatrix}; \quad \begin{bmatrix} Q_x \\ Q_y \end{bmatrix} = \begin{bmatrix} \bar{A}_{11} & 0 \\ 0 & \bar{A}_{22} \end{bmatrix} \begin{bmatrix} \psi_{0,x} \\ \psi_{0,y} \end{bmatrix} \end{aligned} \quad (13)$$

where A and \bar{A} are plate stiffness matrices.

Using Eqs. (12) and (10) in Eq. (8), the area integral is expressed in terms of $\delta u_x, \delta u_y, \delta w_0, \delta \psi_x$ and $\delta \psi_y$. Then applying the Green's theorem wherever required, the terms involving $\delta u_x, \delta u_y, \delta \psi_x, \delta \psi_y, \delta w_{0,x}$ and $\delta w_{0,y}$ in the integrand of Γ_L are expressed in terms of components n, s . It gives forth the following five number of equilibrium equations

$$\begin{aligned}
 & -I_{11}\ddot{u}_{0x} + I_{13}\ddot{w}_{0,x} - I_{15}\ddot{\psi}_{0x} + N_{x,x} + N_{xy,y} = 0 \\
 & -I_{22}\ddot{u}_{0y} + I_{24}\ddot{w}_{0,y} - I_{26}\ddot{\psi}_{0y} + N_{xy,x} + N_{y,y} = 0 \\
 & -I_{31}\ddot{u}_{0,x} + I_{33}\ddot{w}_{0,xx} - I_{35}\ddot{\psi}_{0,x} - I_{42}\ddot{u}_{0,y} + I_{44}\ddot{w}_{0,yy} \\
 & \quad - I_{46}\ddot{\psi}_{0,y} - \bar{I}_{33}\ddot{w}_0 + M_{x,xx} + 2M_{xy,xy} + M_{y,yy} = 0 \\
 & -I_{51}\ddot{u}_{0x} + I_{53}\ddot{w}_{0,x} - I_{55}\ddot{\psi}_{0x} + P_{x,x} + P_{yx,y} - Q_x = 0 \\
 & -I_{62}\ddot{u}_{0y} + I_{64}\ddot{w}_{0,y} - I_{66}\ddot{\psi}_{0y} + P_{xy,x} + P_{y,y} - Q_y = 0
 \end{aligned} \tag{14}$$

The variationally consistent boundary conditions on Γ_L , are obtained by setting separately each of the terms involving $\delta u_{0n}, \delta u_{0s}, \delta w_0, \delta w_{0,n}, \delta \psi_{0n}$ and $\delta \psi_{0s}$ in the boundary integral to zero, since these variations are independent

$$\begin{aligned}
 u_{0n} = \bar{u}_{0n} \quad \text{or} \quad \bar{N}_n = N_n = N_x n_x^2 + N_y n_y^2 + 2N_{xy} n_x n_y, \\
 u_{0s} = \bar{u}_{0s} \quad \text{or} \quad \bar{N}_s = N_s = N_x n_x s_x + N_y n_y s_y + N_{xy} (n_x s_y + n_y s_x), \\
 w_0 = \bar{w}_0 \quad \text{or} \quad (\bar{V}_n + \bar{M}_{ns,s}) = (-I_{31}\ddot{u}_{0x} + I_{33}\ddot{w}_{0,x} - I_{35}\ddot{\psi}_{0x} - I_{37}^j \phi^j) n_x - (I_{42}\ddot{u}_{0y} + I_{44}\ddot{w}_{0,x} \\
 - I_{46}\ddot{\psi}_{0,y}) n_y + (M_{x,x} + M_{xy,y}) n_x + (M_{xy,x} + M_{y,y}) n_y + M_{ns,s}, \\
 w_{0,n} = \bar{w}_{0,n} \quad \text{or} \quad \bar{M}_n = M_n = M_x n_x^2 + M_y n_y^2 + 2M_{xy} n_x n_y, \\
 \psi_{0n} = \bar{\psi}_{0n} \quad \text{or} \quad \bar{P}_n = P_n = P_x n_x^2 + (P_{xy} + P_{yx}) n_x n_y + P_y n_y^2, \\
 \psi_{0s} = \bar{\psi}_{0s} \quad \text{or} \quad \bar{P}_{ns} = P_{ns} = P_x n_x s_x + P_{xy} n_x s_y + P_{yx} n_y s_x + P_y n_y s_y
 \end{aligned}$$

and at corners s_i

$$w_0(s_i) = \bar{w}_0(s_i) \quad \text{or} \quad \Delta M_{ns}(s_i) = \Delta \bar{M}_{ns}(s_i) \tag{15}$$

The boundary conditions considered in this analysis on the edges at $y = \mp b/2$ are as follows

Hard-simply supported (S): $N_y = 0, u_{0x} = 0, w_0 = 0, M_y = 0, P_y = 0, \psi_{0x} = 0,$

Hard-clamped (C): $u_{0y} = 0, u_{0x} = 0, w_0 = 0, w_{0,y} = 0, \psi_{0y} = 0, \psi_{0x} = 0,$ (16)

Free(F): $N_y = 0, N_{yx} = 0, V_y + M_{yx,x} = 0, M_y = 0, P_y = 0, P_{yx} = 0.$

4. Levy-type solution

The boundary conditions at the hard-simply supported edges at $x = 0, a$ are taken as

$$u_{0y} = 0, w_0 = 0, N_x = 0, M_x = 0, P_x = 0, \psi_{0y} = 0 \quad (17)$$

The analytical solution is obtained considering a cross-ply laminate and satisfying the hard-simply supported boundary conditions by taking the solution in terms of Fourier series in x

$$(u_{0y}, w_0, \psi_{0y}, N_x, N_y, M_x, M_y, P_x, P_y, V_y) = \sum_{m=1}^{\infty} \Re[(u_{0y}, w_0, \psi_{0y}, N_x, N_y, M_x, M_y, P_x, P_y, V_y)_m e^{i\omega t}] \sin \bar{m}x \quad (18)$$

$$(u_{0x}, \psi_{0x}, N_{xy}, M_{xy}, P_{xy}, V_x) = \sum_{m=1}^{\infty} \Re[(u_{0x}, \psi_{0x}, N_{xy}, M_{xy}, P_{xy}, V_x)_m e^{i\omega t}] \cos \bar{m}x$$

where $\bar{m} = m\pi/a$ and $(\dots)_m$ denotes the m th Fourier component, a function of y . The solution is obtained in y direction, following the mixed formulation approach, in terms of the twelve primary state variables given as follows

$$X_m = \begin{bmatrix} u_{0x_m}, u_{0y_m}, w_{0m}, w_{0,y_m}, \psi_{0x_m}, \psi_{0y_m}, N_{y_m}, N_{xy_m}, \\ (V_y + M_{xy,x})_m, M_{y_m}, P_{y_m}, P_{xy_m} \end{bmatrix} \quad (19)$$

which appear in the boundaries at edges $y = \mp b/2$. Eq. (18) is substituted into Eqs. (14) and (13), the equilibrium and plate constitutive equations respectively, to yield the system of 12 first order ODEs for the variables X_m for each Fourier component m , as follows

$$\left[H^m \right]_{12 \times 12} \{ X_{m,y} \}_{12 \times 1} = \left[K^m \right]_{12 \times 12} \{ X_m \}_{12 \times 1} \quad (20)$$

The elements of matrix $[H_m]$ and $[K_m]$ are given in Appendix A.

4.1 Frequency and mode shape extraction technique

The general solution of the homogeneous, linear ODEs with constant coefficients given by Eq. (20) is obtained considering its complementary solution $X_m^c = e^{\lambda y} Y_m$ which on substitution into Eq. (20) yields

$$K^m Y_m = \lambda H^m Y_m \Rightarrow M^m Y_m = \lambda Y_m \quad (21)$$

with $M^m = (H^m)^{-1} K^m$. Hence, λ and Y_m are the eigenvalue and the eigenvector pairs of the real matrix M^m . The matrix M^m is first reduced to Hessenberg form and then the eigenvalues and eigenvectors are obtained by the eigenvalue algorithm known as the QR algorithm. The complementary solution is the sum of twelve solutions for the twelve eigenvalues of M^m .

The general solution can be written as

$$X_m = \sum_{j=1}^{12} F_j^m(y) C_j^m \tag{22}$$

where the functions $F_j^m(y)$ depend on the nature of the twelve eigenvalues and the detailed expressions can be found in Ref. (Kumari and Kapuria 2011).

The coefficient matrix F_j^m of Eq. (22) depends on frequency ω_m . For non-trivial solution, its determinant must be zero. First ω_m is bracketed by taking initial guess and can be reckoned by root finding of the equation $\det(F_j^m) = 0$ using the methodology given by Kapuria and Achary (2005). In the general solution of Eq. (22), the twelve number of arbitrary constants are obtained by solving the twelve linear algebraic equations which are yielded using the same number (six each at $y = \mp b/2$) of boundary conditions. After solving for C_j^m , the variables X_m are obtained from Eq. (22). Subsequently, the displacements, stress resultants and hence the stresses are obtained at any point of the plate by using Eqs. (18), (7) and (2) considering a limited number of terms, say M , in the Fourier series.

5. Result and discussion

The best way to assess the accuracy of 2D theories is by comparing with the 3D analytical solutions which do not make any a priori assumptions of field variables through the thickness. Hence, the effectiveness of the present ZIGT in estimating the free vibration behaviors has been investigated for Levy type cross-ply plates by comparison with the other 2D and 3D solutions. The TOT solution can also be obtained using the same number of displacement state variables without requiring any shear correction factor and hence the present TOT results are also compared with the TOT results. Unless mentioned otherwise, the non-dimensional frequency parameter $\bar{\omega}$ considered in the present analysis is as follows: $\bar{\omega} = \omega_m a S \sqrt{\rho_0 / E_2}$, where ω_m is the calculated frequency, S is the span-to-thickness ratio, ρ_0 is the mass density in Kg/m³ and E_2 is the minor elastic modulus in N/m². The dimensionless material parameters used in the present investigation are as follows: $E_1/E_2 = 40$, $E_2 = E_3 = 6.9$ GPa, $G_{12} = G_{13} = 0.6E_2$, $G_{23} = 0.5E_2$, $\nu_{23} = \nu_{13} = \nu_{12} = 0.25$. Any modification to the material constants mentioned above is clearly specified in the relevant places. The plates are designated as per the boundary conditions subjected on the edges at $y = \mp b/2$. A C-S plate, for instance, designates a plate subjected to clamped (C) boundary condition at $y = -b/2$ and simply supported (S) at $y = b/2$. For comparison purpose, the EKM results are transformed to Levy model coordinate system. Hence, the laminate sequence in Ref. (Kumari and Behera 2017) is altered to match with the present model. The percentage errors are calculated with respect to the reference results and is as follows

$$\% \text{ error} = [((2D \text{ frequency}) - (\text{reference frequency})) / (\text{reference frequency})] \times 100$$

The modal displacement and stresses are non-dimensionalized as

$$\bar{v} = \frac{u_{0,y}}{\max(w_0)}; \quad (\bar{\sigma}_y, \bar{\tau}_{yz}) = \frac{Sh(\sigma_y, \tau_{yz})}{E_0 \times \max(w_0)} \quad (23)$$

5.1 Validation

The accuracy of the present ZIGT result has been verified by direct comparison with the 3D exact (Kapuria and Achary 2005) and 3D EKM (Kumari and Behera 2017) results for all round simply supported (S-S) case in Table 1 and with the results of FSDT (Thai *et al.* 2017) and third order shear deformation theory (TSDT) (Hashemi *et al.* 2011) for other type of boundary conditions in Table 2. In Table 1, the dimensionless fundamental natural frequencies (ω) of an un-symmetric two layer [90°/0°] and a symmetric four layer [90°/0°/0°/90°] lay-up cross-ply laminated plates subjected to S-S boundary conditions are presented for S value of (5, 10, 20, 50, 100) and are compared against the reference 3D EKM and 3D exact results. As can be seen from the table that for thin plates the 2D theories have predicted frequencies quite accurately, but for thicker plates, these theories over predict the frequencies. The maximum error being 7.74% for ZIGT and 6.58% for TOT in case of the two-layered thick plate ($S=5$). The error percentage is 1.33% and 0.99%, respectively, for ZIGT and TOT for the four-layered thick plate. The free flexural fundamental frequency of Levy-type single layer isotropic plate is presented in Table 2 and are compared with the TSDT (Hashemi *et al.* 2011) and FSDT (Thai *et al.* 2017) results for different types of boundary conditions. For this table, the frequency parameter $\bar{\omega} = (\omega_m a^2) \sqrt{\rho_0 h / D_1}$, where $D_1 = Eh^3 / 12(1-\nu^2)$ is the flexural rigidity of the plate.

The isotropic material constants are $E = 6.9$ GPa and Poisson's ratio, $\nu = 0.3$. The results are presented for square and rectangular plates for $S = 5$ and 10. It is observed from the table that the ZIGT results are in excellent agreement with the TSDT (Hashemi *et al.* 2011) results for all type of boundary conditions, whereas the FSDT results except for S-S case are erroneous as compared to the higher order theory results. Hereafter, the dimensionless natural frequencies of 3D EKM are given for reference whereas the percentage errors of the present ZIGT and TOT are given for ready assessment.

5.2 Assessment

In this section, the veracity of ZIGT and TOT in predicting free vibration characteristics are assessed against the 3D EKM solution for multilayered composite and sandwich plates. The lowest five flexural frequencies for an un-symmetric two layer [90°/0°] laminated thick ($S=5$) plate is presented in Table 3 for different combination of boundary conditions. The material parameters considered for this table are as follows: $E_1/E_2 = 30$, $G_{12}/E_2 = G_{13}/E_2 = 0.5$, $G_{23}/E_2 = 0.35$, $\nu_{12} = \nu_{13} = 0.3$, $\nu_{23} = 0.49$ with $E_2=6.9$ GPa. It is observed from the table that at lower modes, the % error for S-S case is less as compared to other boundary conditions. The C-C boundary support shows the highest % error i.e., 18.3% and 17.5% for ZIGT and TOT, respectively.

The effect of the span-to-thickness ratio (S) on the fundamental natural frequencies of a three-layer [90°/0°/90°] rectangular plate for boundary conditions C-C, S-C, S-S, F-C, F-S and F-F is presented in Table 4. As observed in Table 4, here also, the % error with respect to 3D EKM frequency is maximum for C-C boundary condition irrespective of plate span-to-thickness ratios ($S=2, 5, 10$). As S value increases, the frequency % error decreases: For S-S case it reduces to

Table 1 Comparison of fundamental natural frequencies for all-round simply-supported (S-S) boundary conditions

Laminate scheme	Theory	S				
		5	10	20	50	100
90°/0°	ZIGT	9.187	10.606	11.116	11.277	11.301
	TOT	9.087	10.568	11.105	11.275	11.300
	3D EKM†	8.526	10.366	11.036	11.263	11.297
	3D Exact‡	8.526	10.366	11.036	11.263	11.297
[90°/0°/0°/90°]	ZIGT	10.830	15.127	17.652	18.673	18.836
	TOT	10.787	15.107	17.647	18.672	18.836
	3D EKM†	10.682	15.068	17.635	18.699	18.835
	3D Exact‡	10.682	15.068	17.635	18.699	18.835

†Kumari and Behera (2017), ‡Kapuria and Achary (2005)

0.03%, whereas for C-C case it reduces to 3.83% for moderately thick (S=10) plate in case of ZIGT prediction.

Effect of inplane elastic modulus ratio (E_1/E_2) on the fundamental natural frequency of an unsymmetrical four layer [90°/0°/90°/0°] moderately thick (S=10) plate is presented in Table 5. It is observed from the table that as the ratio E_1/E_2 decreases thereby making the plate material closer to isotropic condition, the error percentage of 2D theories is decreased, for instance, for $E_1/E_2=40$, the ZIGT and TOT % errors are 1.83% and 2.38% respectively, while for $E_1/E_2=2$ the corresponding errors decreased to -0.14% and -0.11%. Hence, it suggests that the 2D theories perform well for plates made of isotropic materials. The ZIGT results are closer to 3D EKM results than the TOT results for $E_1/E_2=40, 20, 10$ and for $E_1/E_2=2$, the TOT results seem superior to ZIGT.

The percentage errors of the lowest eight flexural frequencies for a three-layer [0°/90°/0°] composite laminated plate is presented in Table 6 for S-S and C-C cases with S=10 and 20 along with the reference 3D EKM results. The non-dimensional frequency parameter $\bar{\omega} = (\omega_m a^2 / \pi^2) \sqrt{\rho_0 h / D_2}$, where $D_2 = E_2 h^3 / 12(1 - \nu_{12} \nu_{21})$. Here in the table, we can see, the 2D theories predict quite accurate results for S-S case and the error percentage is more for C-C case with maximum error 7.36% for the moderately thick plate. The TOT results come more accurate as compared to the ZIGT results both for S-S and C-C cases.

The ZIGT and TOT frequency percentage errors for the lowest five flexural frequencies are presented in Table 7 with respect to the 3D EKM results for a five layered sandwich plate [90°/0°/Core/0°/90°] under five boundary conditions (S-S, C-C, C-S, C-F and F-F) for S = 5, 10 and 20. The material constants those follow are considered for face and core layers, Face: $E_1 = 181$ GPa, $E_2 = E_3 = 10.3$ GPa, $G_{12} = G_{13} = 7.17$ GPa, $G_{23} = 2.87$ GPa, $\nu_{12} = \nu_{13} = 0.28$, $\nu_{23} = 0.33$, $\rho = 1578$ kg/m³, Core: $E_1 = E_2 = 0.276$ GPa, $E_3 = 3.45$ GPa, $G_{13} = G_{23} = 0.414$ GPa, $G_{12} = 0.1104$ GPa, $\nu_{12} = 0.25$, $\nu_{13} = \nu_{23} = 0.02$ and $\rho = 1000$ kg/m³. The frequency parameter $\bar{\omega} = \omega_m a S \sqrt{\rho_0 / E_2}$, where $\rho_0 = 1578$ kg/m³ and $E_2 = 10.3$ GPa. From Table 7, it is clear that the frequency increases with the increase in S value i.e., the thinner the plate, higher the plate frequency. The lowest frequencies are noted for F-F boundary case, while the highest frequencies are noted for C-C boundary case for all

Table 2 Fundamental natural frequency $\bar{\omega} = (\omega_m a^2) \sqrt{\rho_0 h / D_1}$ of square and rectangular single layer isotropic plate for $S=5$ and 10

b/a	S	Theory	S-S	C-C	S-C	F-C	F-S	F-F
1	5	ZIGT	17.447	22.526	19.763	11.370	10.697	8.983
		TSDT (Hashemi <i>et al.</i> 2011)	17.452	22.536	19.770	11.374	10.700	8.984
		FSDT (Thai <i>et al.</i> 2017)	17.449	21.584	19.388	11.573	10.921	9.082
	10	ZIGT	19.060	26.703	22.396	12.249	11.371	9.441
		TSDT (Hashemi <i>et al.</i> 2011)	19.065	26.708	22.402	12.252	11.374	9.442
		FSDT (Thai <i>et al.</i> 2017)	19.065	26.333	22.270	12.366	11.474	9.482
2	5	ZIGT	11.369	12.291	11.780	9.659	9.571	9.089
		TSDT (Hashemi <i>et al.</i> 2011)	11.372	12.294	11.783	9.661	9.573	9.090
		FSDT (Thai <i>et al.</i> 2017)	11.371	12.177	11.736	9.741	9.652	9.150
	10	ZIGT	12.065	13.272	12.591	10.199	10.086	9.551
		TSDT (Hashemi <i>et al.</i> 2011)	12.068	13.275	12.594	10.200	10.087	9.555
		FSDT (Thai <i>et al.</i> 2017)	12.067	13.239	12.580	10.237	10.122	9.577

Table 3 Lowest five flexural frequencies $\bar{\omega} = \omega_m h \sqrt{\rho_0 / E_2}$ for a two layer $[90^\circ/0^\circ]$ laminated composite plate ($S=5$) and the corresponding % error of ZIGT and TOT frequencies (material parameters: $E_1/E_2 = 30$, $G_{12}/E_2 = G_{13}/E_2 = 0.5$, $G_{23}/E_2 = 0.35$, $\nu_{12} = \nu_{13} = 0.3$; = 0.49)

BCs	Theory	Mode sequences				
		1	2	3	4	5
S-S	3D EKM†	0.3117	0.6361	0.6361	0.8532	1.0185
	ZIGT (% error)	6.23	5.72	13.7	4.14	17.1
	TOT (% error)	4.33	5.72	13.7	4.14	13.1
C-C	3D EKM†	0.3782	0.6664	0.6772	0.8819	1.0345
	ZIGT (% error)	15.9	16.4	18.3	0.76	15.3
	TOT (% error)	11.4	11.2	17.5	0.76	14.1
C-F	3D EKM†	0.2328	0.4260	0.5942	0.7107	0.7784
	ZIGT (% error)	6.67	4.28	13.5	13.6	19.2
	TOT (% error)	4.77	4.28	7.97	9.36	13.6
S-F	3D EKM†	0.2179	0.3984	0.4320	0.5893	0.6970
	ZIGT (% error)	6.60	5.05	14.5	11.7	8.12
	TOT (% error)	4.69	3.95	9.21	7.86	12.5
F-F	3D EKM†	0.2073	0.2438	0.5138	0.5763	0.6120
	ZIGT (% error)	7.33	4.82	7.31	16.9	13.6
	TOT (% error)	5.22	3.30	5.28	11.9	9.10

† Kumari and Behera (2017)

the plates. It is to observe that ZIGT predicts quite accurate results for S-S and F-F boundary conditions, but for other type of boundary conditions it gives more error and the maximum (4.41%) being for C-C boundary case. It is observed that for sandwich plate ZIGT predicts superior results than TOT for all types of boundary conditions and plate categories.

Table 4 Effect of span-to-thickness ratio (S) on the fundamental natural frequencies of a three layer $[90^\circ/0^\circ/90^\circ]$ laminated composite plate: (material parameters: $E_1/E_2 = 40$, $E_2 = E_3 = 6.9$ GPa, $G_{12} = G_{13} = 0.6E_2$, $G_{23} = 0.5E_2$, $\nu_{13} = \nu_{12} = 0.25$, $\nu_{23} = 0.49$)

Theory	S	C-C	S-C	S-S	F-C	F-S	F-F
3D EKM†		5.331	5.201	5.192	3.481	3.072	2.715
HSDT‡(% error)	2	-0.48	-2.51	-0.77	3.50	4.79	7.30
ZIGT (% error)		34.0	18.9	5.47	9.21	4.35	5.99
TOT (% error)		26.7	14.5	3.30	6.94	2.73	3.73
3D EKM†		11.426	10.679	10.246	5.81	4.401	3.911
HSDT‡(% error)	5	-0.05	-2.64	-0.88	1.19	2.36	3.03
ZIGT (% error)		6.11	5.75	0.53	3.20	2.25	2.95
TOT (% error)		6.11	4.57	0.19	2.59	1.66	2.21
3D EKM†		19.66	17.108	14.702	7.135	4.876	4.241
HSDT‡(% error)	10	0.15	-1.00	-0.29	0.37	0.69	1.72
ZIGT (% error)		3.83	2.17	0.03	0.89	0.76	0.77
TOT (% error)		3.14	1.81	0.00	0.76	0.59	0.57

†Kumari and Behera (2017), ‡Khdeir and Librescu (1988)

Table 5 Effect of inplane modulus ratio (E_1/E_2) on the fundamental natural frequency of an unsymmetrical four layer $[90^\circ/0^\circ/90^\circ/0^\circ]$ laminated composite plate ($S=10$)

Theory	E_1/E_2	S-S	C-C	C-S	C-F
3D EKM†		0.14501	0.18652	0.1649	0.10875
ZIGT (% error)	40	1.83	5.30	3.58	1.98
TOT (% error)		2.38	6.37	4.40	-6.32
3D EKM†		0.11653	0.16088	0.13738	0.08638
ZIGT (% error)	20	0.79	2.97	1.75	0.57
TOT (% error)		1.10	3.72	2.26	0.86
3D EKM†		0.09438	0.13627	0.11337	0.06869
ZIGT (% error)	10	0.22	0.98	0.49	-0.41
TOT (% error)		0.38	1.44	0.78	-0.26
3D EKM†		0.06719	0.09641	0.07992	0.04628
ZIGT (% error)	2	-0.14	-1.94	-1.08	-3.41
TOT (% error)		-0.11	-1.85	-1.02	-3.38

†Kumari and Behera (2017)

The distributions of inplane displacement \bar{v} , normal stress $\bar{\sigma}_y$, and shear stress $\bar{\tau}_{yz}$ for S-S boundary condition are illustrated in Fig. 2 for moderately thick ($S=10$) and thick ($S=5$) sandwich plates for the first mode ($m=1$). The ZIGT and TOT predictions are compared with the 3D exact and 3D EKM predictions and found that ZIGT has fairly accurate predictions while the TOT over predicts \bar{v} for the thick plate and $\bar{\tau}_{yz}$ for both thick and moderately thick plates. Fig. 3 displays the variation of displacement and stress variables for (a) C-C and (b) C-F boundary conditions. From the figures, it is observed that ZIGT and TOT predict erroneous results while the ZIGT predictions are superior to the TOT predictions.

Table 6 Lowest eight natural frequencies, of the 3D EKM with the % errors of ZIGT and TOT results for a three ply [90°/0°/90°] laminated plate for S-S and C-C boundary conditions

BCs	S	Theory	Mode sequences							
			1	2	3	4	5	6	7	8
S-S	10	3D EKM†	5.154	7.606	12.276	13.100	14.355	17.399	18.087	21.355
		FSDT‡(% error)	0.22	1.98	5.21	-0.39	0.14	2.24	7.82	-1.42
		ZIGT (% error)	0.07	1.50	3.94	0.36	0.64	2.03	5.72	0.58
		TOT (% error)	0.04	1.11	2.89	0.09	0.31	1.35	4.08	-0.22
	20	3D EKM†	6.131	8.841	14.845	19.32	20.618	23.287	24.202	30.426
		FSDT‡(% error)	0.12	0.53	1.79	0.18	0.23	3.36	0.59	1.98
		ZIGT (% error)	0.01	0.41	1.46	0.03	0.07	2.69	0.35	1.50
		TOT (% error)	0.01	0.31	1.12	0.02	0.04	2.05	0.21	1.11
C-C	10	3D EKM†	5.796	9.019	13.363	13.83	15.147	18.521	19.487	21.535
		FSDT‡(% error)	1.30	4.82	-0.17	7.58	1.27	3.82	8.95	-1.21
		ZIGT (% error)	0.97	3.91	0.51	6.14	1.53	3.42	7.36	-0.27
		TOT (% error)	0.74	3.05	0.21	4.77	1.02	2.52	5.66	-1.05
	20	3D EKM†	6.867	11.04	18.001	19.578	21.675	26.23	26.827	33.205
		FSDT‡(% error)	0.33	1.87	3.68	0.21	0.58	1.75	5.34	3.44
		ZIGT (% error)	0.21	1.55	3.05	0.06	0.37	1.35	4.37	2.81
		TOT (% error)	0.16	1.22	2.41	0.04	0.27	1.04	3.43	2.81

†Kumari and Behera (2017) and ‡Liew (1996)

Table 7 The % errors of lowest five flexural natural frequencies of ZIGT and TOT with respect to 3D EKM for a square sandwich plate under five different boundary conditions for S=5, 10 and 20

S	Mode	S-S			C-C			C-S			C-F			F-F		
		3D EKM†	ZIGT %error	TOT %error	3D EKM†	ZIGT %error	TOT %error	3D EKM†	ZIGT %error	TOT %error	3D EKM†	ZIGT %error	TOT %error	3D EKM†	ZIGT %error	TOT %error
5	1	4.807	0.07	7.03	5.041	2.29	8.99	4.876	1.53	8.41	3.605	0.51	9.09	3.181	0.12	9.94
	2	7.921	0.09	-2.21	8.036	1.00	10.8	7.958	0.66	10.5	6.162	2.32	8.09	3.829	0.29	8.21
	3	8.367	0.14	5.77	8.397	4.41	9.53	8.388	2.20	7.59	7.232	0.26	7.10	6.997	0.29	10.7
	4	10.479	0.14	7.87	10.507	2.89	10.2	10.497	1.46	9.01	8.890	1.36	10.0	7.637	0.25	2.47
	5	11.505	0.13	3.57	11.564	0.59	3.04	11.525	0.41	3.39	10.278	1.01	5.88	7.972	0.51	5.90
10	1	7.677	0.04	4.36	8.821	1.30	6.14	8.201	0.82	5.46	5.597	0.25	5.39	4.951	0.14	4.69
	2	14.164	0.05	8.78	14.702	0.55	9.09	14.406	0.34	8.99	10.323	1.22	5.56	5.791	0.13	5.41
	3	15.078	0.08	4.66	15.469	2.25	6.91	15.296	1.18	5.81	13.005	0.55	6.66	12.728	0.07	8.98
	4	19.228	0.07	7.03	19.508	1.51	8.39	19.381	0.79	7.71	15.915	0.70	8.54	13.146	0.15	3.90
	5	21.437	0.07	5.06	21.726	0.31	3.67	21.567	0.21	4.43	18.388	1.34	5.82	13.486	0.12	2.86
20	1	9.849	0.02	1.73	13.453	0.58	3.33	11.569	0.30	2.50	7.009	0.19	2.18	6.193	0.01	0.68
	2	21.707	0.03	5.27	23.338	0.42	5.52	22.460	0.16	5.31	14.973	0.55	2.93	7.249	0.09	2.23
	3	23.314	0.04	2.68	26.275	1.05	4.64	24.875	0.63	3.79	20.240	0.15	3.59	17.551	0.04	1.73
	4	30.711	0.03	4.35	32.819	0.77	5.41	31.811	0.40	4.88	24.870	0.32	5.18	19.823	-1.01	4.59
	5	36.632	0.05	3.49	37.517	0.18	1.05	37.031	0.11	2.37	29.958	0.53	3.69	20.765	0.08	0.95

†Kumari and Behera (2017)

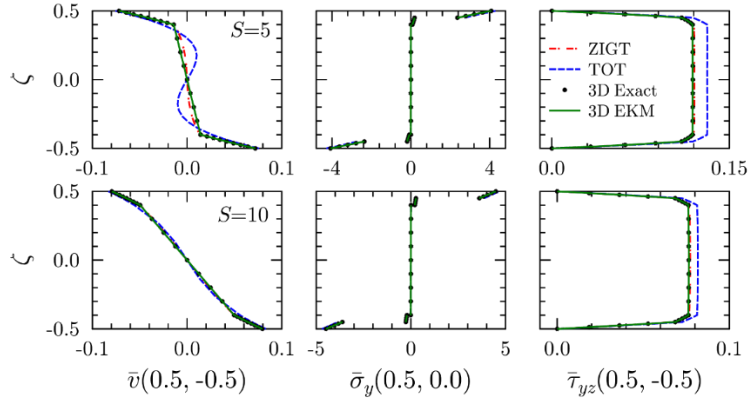
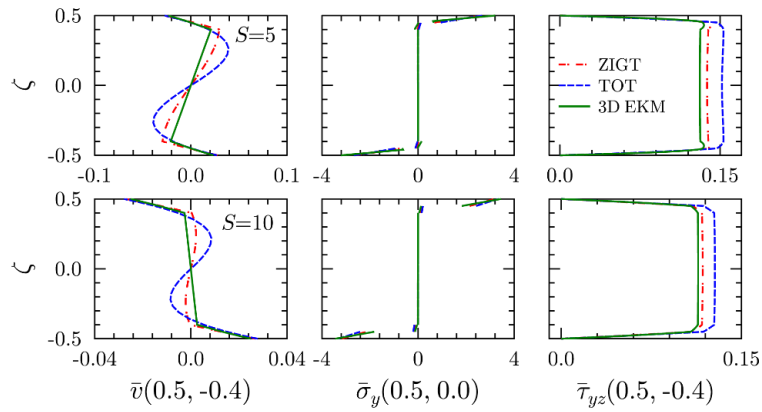
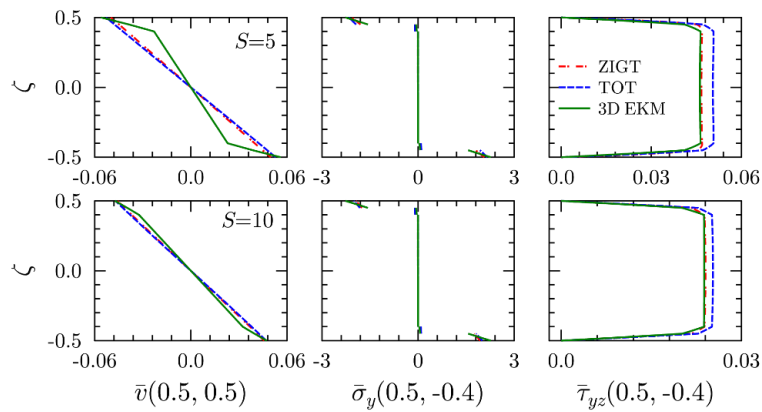


Fig. 2 Distributions \bar{v} , $\bar{\sigma}_y$ and $\bar{\tau}_{yz}$ for the first mode of all round simply supported (S-S) square sandwich plate



(a) Clamped-Clamped (C-C)



(b) Clamped-Free (C-F)

Fig. 3 Distributions \bar{v} , $\bar{\sigma}_y$ and $\bar{\tau}_{yz}$ for the first modes of square sandwich plate for C-C and C-F boundary conditions

6. Conclusions

The assessment of zig-zag theory for the free vibration of a single layer isotropic, laminated composite and sandwich plates has been carried out for symmetric and un-symmetric cross-ply lay-ups, different plate thicknesses and various boundary conditions.

- The 2D theories predict accurate frequencies for the simply supported case, but for other boundary conditions, 2D theories predict erroneous results even in the first mode frequency. The percentage error is observed maximum for C-C boundary condition for all plate configurations. The error in the ZIGT results for natural frequencies is large for thicker plates.

- It is observed that TOT produces better natural frequencies than ZIGT for symmetric laminates, but for unsymmetrical laminated and sandwich plates, ZIGT predicts the frequency for different boundary conditions within 3% error with respect to 3D elasticity solution while TOT gives 10% error.

- As the inplane elastic modulus ratio decreases, thereby making the plate material closer to isotropic condition, the frequency percentage errors of 2D theories with respect to the 3D EKM also decrease.

- The comparison of displacement and stresses for sandwich plate shows that ZIGT predicts quite accurately than the TOT for S-S case, but for C-C and C-F cases both theories estimate highly erroneous results. The displacement profile predicted by TOT is far from the exact prediction.

The natural frequencies tabulated in this paper will be handy for the research community to evaluate the accuracy of the different finite element models and 2D laminate theories. The present zig-zag theory can be recommended for dynamic analysis of composite and sandwich plates for its firmness, accuracy and computational efficiency.

References

- Akavci, S.S. and Tanrikulu, A.H. (2008), "Buckling and free vibration analyses of laminated composite plates by using two new hyperbolic shear-deformation theories", *Mech. Compos. Mater.*, **44**(2), 145-154.
- Caliri Jr., M.F., Ferreira, A.J.M. and Tita, V. (2016), "A review on plate and shell theories for laminated and sandwich structures highlighting the finite element method", *Compos. Struct.*, **156**, 63-77.
- Chen, W.C. and Liu, W.H. (1990), "Deflections and free vibrations of laminated plates-Levy type solutions", *J. Mech. Sci.*, **32**(9), 779-793.
- Ferreira, A.J.M., Castro, L.M.S. and Bertoluzza, S. (2009), "A high order collocation method for the static and vibration analysis of composite plates using a first-order theory", *Compos. Struct.*, **89**(3), 424-432.
- Ferreira, A.J.M., Roque, C.M.C. and Jorge, R.M.N. (2005), "Free vibration analysis of symmetric laminated composite plates by FSDT and radial basis functions", *Comput. Method. Appl. M.*, **194**(39), 4265-4278.
- Hashemi, S.H. and Arsanjani, M. (2005), "Exact characteristic equations for some of classical boundary conditions of vibrating moderately thick rectangular plates", *J. Solids Struct.*, **42**(3-4), 819-853.
- Hashemi, S.H., Fadaee, M. and Taher, H.R.D. (2011), "Exact solutions for free flexural vibration of Levy-type rectangular thick plates via third-order shear deformation plate theory", *Appl. Math. Modell.*, **35**(2), 708-727.
- Kant, T. and Swaminathan, K. (2001), "Analytical solutions for free vibration of laminated composite and sandwich plates based on a higher-order refined theory", *Compos. Struct.*, **51**(1), 73-85.
- Kapurja, S. and Achary, G.G.S. (2005), "Exact 3D piezoelectricity solution of hybrid cross - ply plates with damping under harmonic electro-mechanical loads", *J. Sound Vib.*, **282**(3-5), 617-634.
- Kapurja, S. and Kulkarni, S.D. (2007), "An improved discrete Kirchhoff quadrilateral element based on

- third-order zigzag theory for static analysis of composite and sandwich plates”, *J. Numer. Meth. Eng.*, **69**(9), 1948-1981.
- Karama, M. (1993), “An evaluation of the edge solution for a higher-order laminated plate theory”, *Compos. Struct.*, **25**(1-4), 495-502.
- Khdeir, A.A. (1988), “Free vibration and buckling of symmetric cross-ply laminated plates by an exact method”, *J. Sound Vib.*, **126**(3), 447-461.
- Khdeir, A.A. (1989), “Free vibration and buckling of unsymmetric cross-ply laminated plates using a refined theory”, *J. Sound Vib.*, **128**(3), 377-395.
- Khdeir, A.A. and Librescu, L. (1988), “Analysis of symmetric cross-ply laminated elastic plates using a higher-order theory: Part II-Buckling and free vibration”, *Compos. Struct.*, **9**(4), 259-277
- Kumari, P. and Behera, S. (2017), “Three-dimensional free vibration analysis of levy-type laminated plates using multi-term extended Kantorovich method”, *Compos. Part B: Eng.*, **116**, 224-238.
- Kumari, P. and Kapuria, S. (2011), “Boundary layer effects in rectangular cross-ply Levy-type plates using zigzag theory”, *ZAMM/J. Appl. Math. Mech.*, **91**(7), 565-580.
- Leissa, A.W. (1973), “The free vibration of rectangular plates”, *J. Sound Vib.*, **31**(3), 257-293.
- Leissa, A.W. and Kang, J.H. (2002), “Exact solutions for vibration and buckling of an SS-C-SS-C rectangular plate loaded by linearly varying in-plane stresses”, *J. Mech. Sci.*, **44**(9), 1925-1945.
- Liew, K.M. (1996), “Solving the vibration of thick symmetric laminates by Reissner/Mindlin plate theory and the p-Ritz method”, *J. Sound Vib.*, **198**(3), 343-360.
- Mahi, A., Bedia, E.A.A. and Tounsi, A. (2015), “A new hyperbolic shear deformation theory for bending and free vibration analysis of isotropic functionally graded sandwich and laminated composite plates”, *Appl. Math. Model.*, **39**(9), 2489-2508.
- Mantari, J.L., Oktem, A.S. and Guedes, S.C. (2011), “Static and dynamic analysis of laminated composite and sandwich plates and shells by using a new higher-order shear deformation theory”, *Compos. Struct.*, **94**(1), 37-49.
- Matsunaga, H. (2000), “Vibration and stability of cross-ply laminated composite plates according to a global higher-order plate theory”, *Compos. Struct.*, **48**(4), 231-244.
- Matsunaga, H. (2001), “Vibration and stability of angle-ply laminated composite plates subjected to in-plane stresses”, *J. Mech. Sci.*, **43**(8), 1925-1944.
- Meiche, N.E., Tounsi, A., Ziane, N., Mechab, I. and Bedia, E.A.A. (2011), “A new hyperbolic shear deformation theory for buckling and vibration of functionally graded sandwich plate”, *J. Mech. Sci.*, **53**(4), 237-247.
- Mindlin, R.D. (1951), “Influence of rotary inertia and shear on flexural motions of isotropic elastic plates”, *J. Appl. Mech.*, **18**(1), 31-38.
- Noor, A.K. (1973), “Free vibrations of multilayered composite plates”, *AIAAJ.*, **11**(7), 1038-1039.
- Reissner, E. (1945), “The effect of transverse shear deformation on the bending of elastic plates”, *J. Appl. Mech.*, **12**(2), 69-77.
- Sayyad, A.S. and Ghugal, Y.M. (2015), “On the free vibration analysis of laminated composite and sandwich plates: A review of recent literature with some numerical results”, *Compos. Struct.*, **129**, 177-201.
- Sayyad, A.S. and Ghugal, Y.M. (2017), “Bending, buckling and free vibration of laminated composite and sandwich beams: A critical review of literature”, *Compos. Struct.*, **171**, 486-504.
- Swaminathan, K. and Patil, S.S. (2008), “Analytical solutions using a higher order refined computational model with 12 degrees of freedom for the free vibration analysis of anti-symmetric angle-ply plates”, *Compos. Struct.*, **82**(2), 209-216.
- Thai, H.T. and Choi, D.H. (2013), “A simple first-order shear deformation theory for laminated composite plates”, *Compos. Struct.*, **106**, 754-763.
- Thai, H.T. and Kim, S.E. (2012), “Levy-type solution for free vibration analysis of orthotropic plates based on two variable refined plate theory”, *Appl. Math. Modell.*, **36**(8), 3870-3882.
- Thai, H.T., Nguyen, T.K., Vo, T.P. and Ngo, T. (2017), “A new simple shear deformation plate theory”, *Compos. Struct.*, **171**, 277-285.

Xiang, Y. and Wei, G.W. (2004), "Exact solutions for buckling and vibration of stepped rectangular Mindlin plates", *J. Solids Struct.*, **41**(1), 279-294.

CC

Appendix A

$$H^m = \begin{bmatrix} A_{3,3} & 0 & 0 & 0 & A_{3,8} & 0 & 0 & 0 & 0 & 0 & 0 & 0 \\ 0 & A_{2,2} & 0 & -A_{2,5} & 0 & A_{2,10} & 0 & 0 & 0 & 0 & 0 & 0 \\ 0 & 0 & 1 & 0 & 0 & 0 & 0 & 0 & 0 & 0 & 0 & 0 \\ 0 & A_{5,2} & 0 & -A_{5,5} & 0 & A_{5,10} & 0 & 0 & 0 & 0 & 0 & 0 \\ A_{3,8} & 0 & 0 & 0 & A_{8,8} & 0 & 0 & 0 & 0 & 0 & 0 & 0 \\ 0 & A_{10,2} & 0 & -A_{10,5} & 0 & A_{10,10} & 0 & 0 & 0 & 0 & 0 & 0 \\ 0 & 0 & 0 & 0 & 0 & 0 & 1 & 0 & 0 & 0 & 0 & 0 \\ 0 & \bar{m}A_{1,2} & 0 & -\bar{m}A_{1,5} & 0 & \bar{m}A_{1,10} & 0 & 1 & 0 & 0 & 0 & 0 \\ 0 & -\bar{m}^2 A_{4,2} & 0 & \bar{m}^2 A_{4,5} & 0 & -\bar{m}^2 A_{4,10} & 0 & 0 & 1 & 0 & 0 & 0 \\ -2\bar{m}A_{6,3} & 0 & 0 & 0 & -2\bar{m}A_{6,8} & 0 & 0 & 0 & 0 & 1 & 0 & 0 \\ -\bar{m}A_{9,3} & 0 & 0 & 0 & -\bar{m}A_{9,8} & 0 & 0 & 0 & 0 & 0 & 1 & 0 \\ 0 & \bar{m}A_{7,2} & 0 & -\bar{m}A_{7,5} & 0 & \bar{m}A_{7,10} & 0 & 0 & 0 & 0 & 0 & 1 \end{bmatrix} \quad (A.1)$$

$$K^m = \begin{bmatrix} K^a & K^b \end{bmatrix} \quad (A.2)$$

$$K^m = \begin{bmatrix} 0 & -\bar{m}A_{3,3} & 0 & 2\bar{m}A_{3,6} & 0 & -\bar{m}A_{3,9} \\ \bar{m}A_{2,1} & 0 & -\bar{m}^2 A_{2,4} & 0 & \bar{m}A_{2,7} & 0 \\ 0 & 0 & 0 & 1 & 0 & 0 \\ \bar{m}A_{5,1} & 0 & -\bar{m}^2 A_{5,4} & 0 & \bar{m}A_{5,7} & 0 \\ 0 & -\bar{m}A_{8,3} & 0 & 2\bar{m}A_{8,6} & 0 & -\bar{m}A_{8,9} \\ \bar{m}A_{10,1} & 0 & -\bar{m}^2 A_{10,4} & 0 & \bar{m}A_{10,7} & 0 \\ 0 & 0 & 0 & 0 & 0 & 0 \\ \bar{m}^2 A_{1,1} & 0 & -\bar{m}^3 A_{1,4} & 0 & \bar{m}^2 A_{1,7} & 0 \\ -\bar{m}^3 A_{4,1} & 0 & -\bar{m}^4 A_{4,4} & 0 & -\bar{m}^3 A_{4,7} & 0 \\ 0 & 2\bar{m}^2 A_{6,8} & 0 & -4\bar{m}^2 A_{6,6} & 0 & 2\bar{m}^2 A_{6,9} \\ 0 & \bar{m}^2 A_{9,3} & 0 & -2\bar{m}^2 A_{9,6} & 0 & 2\bar{m}^2 A_{9,9} + \bar{A}_{22} \\ \bar{m}^2 A_{7,1} & 0 & -\bar{m}^3 A_{7,4} & 0 & \bar{m}^2 A_{7,7} + \bar{A}_{11} & 0 \end{bmatrix} \quad (A.3)$$

and the non-zero elements of K^b are

$$K_{1,8} = K_{2,7} = K_{4,10} = K_{5,12} = K_{6,11} = K_{10,9} = 1, \quad K_{7,8} = \bar{m} \quad (A.4)$$

where $\bar{m} = m\pi / a$.

The non-zero elements from the contribution of dynamic terms of matrix Km with addition to the above

$$\begin{aligned}
K_{7,2}^m &= -\omega^2 I_{22} & K_{7,4}^m &= \omega^2 I_{24} & K_{7,6}^m &= -\omega^2 I_{26} & K_{8,1}^m &= -\omega^2 I_{11}, \\
K_{8,3}^m &= \bar{m}\omega^2 I_{13} & K_{8,5}^m &= -\omega^2 I_{15} & K_{9,1}^m &= \bar{m}\omega^2 I_{31} & K_{9,3}^m &= -\bar{m}^2 \omega^2 I_{33} - \omega^2 \bar{I}_{33} \\
K_{9,5}^m &= \bar{m}\omega^2 I_{35} & K_{10,2}^m &= -\omega^2 I_{42} & K_{10,4}^m &= \omega^2 I_{44} & & \\
K_{10,6}^m &= -\omega^2 I_{46} & K_{11,2}^m &= -\omega^2 I_{62} & K_{11,4}^m &= \omega^2 I_{64} & K_{11,6}^m &= -\omega^2 I_{66} \\
K_{12,1}^m &= -\omega^2 I_{51} & K_{12,3}^m &= \bar{m}\omega^2 I_{53} & K_{12,5}^m &= -\omega^2 I_{55} & &
\end{aligned} \tag{A.5}$$